

# UC San Diego

## UC San Diego Previously Published Works

### Title

Progression of muscle loss and fat accumulation in a rabbit model of rotator cuff tear.

### Permalink

<https://escholarship.org/uc/item/9r68r30q>

### Journal

Journal of orthopaedic research : official publication of the Orthopaedic Research Society, 40(5)

### ISSN

0736-0266

### Authors

Vargas-Vila, Mario A  
Gibbons, Michael C  
Wu, Isabella T  
[et al.](#)

### Publication Date

2022-05-01

### DOI

10.1002/jor.25160

Peer reviewed



Published in final edited form as:

*J Orthop Res.* 2022 May ; 40(5): 1016–1025. doi:10.1002/jor.25160.

## Progression of Muscle Loss and Fat Accumulation in a Rabbit Model of Rotator Cuff Tear

Mario A. Vargas-Vila, MD, PhD<sup>1</sup>, Michael C. Gibbons, PhD<sup>2</sup>, Isabella T. Wu, MD, MPH<sup>1</sup>, Mary C. Esparza, BS<sup>1</sup>, Kenji Kato, MD, PhD<sup>3</sup>, Seth D. Johnson, BS<sup>1</sup>, Koichi Masuda, MD<sup>1</sup>, Samuel R. Ward, PT, PhD<sup>1,2,4</sup>

<sup>1</sup>Department of Orthopaedic Surgery, UC San Diego, La Jolla CA, USA

<sup>2</sup>Department of Bioengineering, UC San Diego, La Jolla CA, USA

<sup>3</sup>Department of Orthopaedic Surgery, Nagoya City University, Nagoya, Japan

<sup>4</sup>Department of Radiology, UC San Diego, La Jolla CA, USA

### Abstract

Rotator cuff (RC) tears present a treatment challenge due to muscle atrophy and degeneration, fatty infiltration, and fibrosis. The purpose of this study was to generate a high time-resolution model of RC tear in rabbits, and to characterize the progression of architectural and histological changes. Thirty-five female New Zealand White rabbits (age: 6 months) underwent left supraspinatus tenotomy. Five rabbits were used to evaluate immediate muscle architectural changes. The remaining 30 rabbits underwent right shoulder sham surgery and sacrifice at 1, 2, 4, 8, or 16 weeks. Histology was used to quantify muscle fiber cross-sectional area (CSA), muscle degeneration and regeneration, and fat localized to inter- versus intra-fascicular regions. Muscle fiber CSA decreased by 26.5% compared to sham at 16 weeks (effect of treatment,  $p < 0.0001$ ). Muscle degeneration increased after tenotomy (effect of treatment,  $p = 0.0006$ ) without any change in regeneration. Collagen and fat content increased by 4 weeks and persisted through 16 weeks. Inter-fascicular fat was increased at all time points, but intra-fascicular fat was increased only at

---

**Corresponding Author:** Samuel R. Ward, PT, PhD, Professor and Vice Chair of Research, Departments of Orthopaedic Surgery, Radiology, and Bioengineering, UC San Diego, 9500 Gilman Drive (0863), La Jolla, CA 92093-0863, Tel: +1 858 534 4918; Fax: +1 858 822 3807; s1ward@health.ucsd.edu.

Author Contributions Statement:

MAV: substantial contributions to research design; acquisition, analysis or interpretation of data; and drafting the paper or revising it critically

MCG: substantial contributions to research design; acquisition, analysis or interpretation of data; and drafting the paper or revising it critically

ITW: substantial contributions to acquisition, analysis or interpretation of data; and drafting the paper or revising it critically

MCE: substantial contributions to research design; acquisition, analysis or interpretation of data; and drafting the paper or revising it critically

KK: substantial contributions to research design; acquisition, analysis or interpretation of data; and drafting the paper or revising it critically

SDJ: substantial contributions to research design; acquisition, analysis or interpretation of data; and drafting the paper or revising it critically

KM: substantial contributions to research design; acquisition, analysis or interpretation of data; and drafting the paper or revising it critically

SRW: substantial contributions to research design; acquisition, analysis or interpretation of data; and drafting the paper or revising it critically

All authors reviewed and approved of the final submitted manuscript version.

1, 4, and 16 weeks post-tenotomy. Intra-fascicular fat adjacent to degenerating muscle fibers increased as well (effect of treatment,  $p < 0.0001$ ; effect of time,  $p = 0.0102$ ).

### Key Terms:

Shoulder; rotator cuff; Muscle injuries; Muscle physiology

---

## Introduction

The prevalence of rotator cuff (RC) tears in the general population, and particularly in the aged population<sup>1</sup>, represents a substantial burden to the healthcare system and patient quality of life<sup>2</sup>. Despite advances in surgical techniques and technology, rotator cuff tears remain one of the most difficult orthopedic injuries to treat. Surgical intervention is generally successful at reducing pain and improving function<sup>3</sup>. However, reversing negative changes in the muscle, avoiding re-tear, and restoring function remain significant clinical challenges, particularly in patients with chronic, massive tears<sup>3-5</sup>. Contemporary research is now attempting to identify the cellular and molecular mechanisms that drive muscle loss and fat accumulation in human RC muscles. To this end, several animal models, including mouse<sup>6; 7</sup>, rat<sup>6; 8</sup>, rabbit<sup>9; 10</sup>, and sheep<sup>11; 12</sup>, have been developed to study pathophysiological mechanisms of RC disease, and a growing number of studies have evaluated potential therapeutic approaches in these models<sup>13-17</sup>.

As our clinical understanding of RC disease evolves, the ideal animal model should reflect the aspects of disease progression that continue to present treatment challenges. Recent evidence suggests that not just muscle atrophy and pericellular fat deposition, but muscle degeneration<sup>18; 19</sup>—in which muscle fibers are damaged<sup>20</sup> and possibly replaced by fat<sup>18</sup>—is a key feature of the most intractable cases of RC tear<sup>18</sup>. The degenerative state is distinguishable from load- or demand-mediated atrophy by high degrees of inflammatory cells, connective tissue, and altered vascularization<sup>18; 19</sup>. Additionally, “fatty atrophy” and “fatty infiltration” are widely discussed in the RC literature, but evidence suggesting direct “fatty replacement” of muscle by lipid within a preserved muscle matrix architecture has only emerged very recently<sup>18</sup>. To date, these phenomena have not been explicitly described in any animal model. Based on existing studies, the mouse and rat models do not seem to develop the degree of muscle atrophy, degeneration, or cell-level fat replacement found in humans, even with the controversial addition of a nerve injury<sup>6-8</sup>. At the other end of the spectrum, the sheep does seem to lose muscle and accumulate fat similarly to humans<sup>11; 21</sup>, but the size of the sheep and its associated costs limit its widespread use. Therefore, the rabbit is an attractive alternative at an intermediate size and cost, provided it adequately recapitulates the pathological phenotype found in human disease.

Indeed, a limited number of rabbit models of RC disease have been developed and deployed for both basic science<sup>9; 10</sup> and translational<sup>14; 16</sup> purposes. These studies have demonstrated robust muscle atrophy and accumulation of fat in rabbit RC<sup>9; 10; 22; 23</sup>, but the development of muscle degeneration/regeneration and the relative localization of accumulated adipocytes in the rabbit RC has yet to be explored in detail. Only one recent study has attempted to

isolate and quantify inter- versus intra-fascicular fat at 6 and 12 weeks post-tenotomy<sup>24</sup>. Given ongoing investigation into the role of intra-fascicular lipid accumulation in the development and progression of human RC pathology<sup>18–20; 25</sup>, understanding the expected progression of these changes is critical in this pre-clinical model. Additionally, the timecourse has not been explored in sufficient detail to identify the correct timing to explore mechanisms of muscle degeneration or fat accumulation, or to test the ability of adjuvant therapies to reverse these processes. Earlier studies sacrificed or tested animals starting at 6 weeks<sup>9; 10; 23; 24; 26</sup>, but more recent data suggests that muscle and fat changes at 2–4 weeks may better represent a repairable, Goutallier stage 2 tear model<sup>27</sup>. As such, the purpose of this study was to generate a high time-resolution, repeatable tenotomy model of RC tear in the rabbit, and to characterize the time course of atrophy, degeneration, fat accumulation, and fibrosis. The short-term goal is to implement this model for the biological exploration of muscle cell degeneration and testing of therapeutic interventions.

## Methods

### Animals

A total of 35 female New Zealand White rabbits were used for this study: 5 to characterize muscle architecture immediately after tenotomy, and 30 to evaluate post-tenotomy changes over time. All protocols were approved by the University of California, San Diego Institutional Animal Care and Use Committee (protocol #S11246), and all animals were approximately 6 months of age at the start of the study. Cage locations were assigned upon arrival, each rabbit was given a number ID, and then randomized to one of the study groups. Researchers were aware of the allocation during the surgeries and tissue harvest, but the specimens were identified by ID number only. Animals were single-housed with food and water ad lib, environmental and food enrichment, and visual access to other animals. There were no adverse events in this study and no animals met the criteria for humane endpoints. These criteria included: displaying clinical signs of disease, loss of appetite, weight below 15% of what is expected for the animal, and/or signs of distress, such as self-mutilation.

### Surgical Procedures

For surgical procedures, anesthesia was induced with a subcutaneous injection of ketamine and xylazine, rabbits were intubated, and anesthesia was maintained with a 2–4% isoflurane vapor. Tenotomy of the supraspinatus was performed unilaterally by sharp transection of the supraspinatus tendon at its footprint on the greater tubercle of the humerus, followed by blunt dissection of surrounding soft tissue connections to allow unhindered retraction of the tendon stump and distal pole of the muscle. For the 5 “muscle architecture” rabbits, the contralateral shoulder remained an unoperated internal control, and euthanasia was performed immediately following tenotomy via intravenous pentobarbital (Beuthanasia) overdose. In the remaining 30 “time series” animals, a Penrose drain was secured to the tendon stump to prevent scar formation between the tendon and surrounding soft tissue, while a sham operation was performed on the contralateral side. Postoperatively, a fentanyl patch was placed on the back of the animal to help alleviate pain for 3 days. A behavioral assessment for pain was performed daily for 2 weeks postoperatively. The “time series”

animals were euthanized at 1, 2, 4, 8, or 16 weeks (n=6 per time point) to study the time course of pathological changes in the RC muscle following tenotomy.

### Architecture Animals

Immediately after tenotomy and sacrifice, the humerus was transected and the scapula with associated musculature was removed en bloc, in order to preserve the muscle architecture and native configuration of the glenohumeral joint at a 90° angle. Then retraction distance was measured as the distance from the footprint of the supraspinatus tendon on the greater tubercle of the humerus to the tendon stump. Pennation angle was measured for each of four regions: anterior lateral (A1), anterior medial (A2), posterior lateral (P1), and posterior medial (P2), where the central tendon was used to demarcate the muscle midline and the division between anterior and posterior regions. The joint was pinned with the humerus at a 90° angle to the scapular spine and submersion fixed in 10% formalin for one week. The supraspinatus muscle was then harvested from scapula, and fascicles were dissected from each region of the muscle as a proxy for fiber length. Fiber bundles were dissociated from these fascicles and sarcomere length was measured using established laser diffraction techniques<sup>28</sup>.

### Time Series Animals

At each time point from 1 to 16 weeks post-tenotomy, both the operated and sham shoulders were resected, and the retraction distance (with the joint in a similar 90° position) was recorded for the tenotomized muscle. Both supraspinatus muscles were harvested, and a full-muscle thickness segment was dissected from each of the regions described above, combined accounting for approximately 60–75% of the total muscle. These segments were then pinned to *in vivo* length, and snap frozen in liquid nitrogen-cooled isopentane before being stored at –80° C. Frozen muscle segments were then embedded in OCT and sectioned in a cryostat to obtain both axial and longitudinal sections.

### Myosin Heavy Chain Isoforms

Myosin heavy chain (MHC) content was analyzed from whole muscle sections that were frozen for histology by using sodium dodecyl sulfate-polyacrylamide gel electrophoresis (SDS-PAGE), as described previously<sup>29</sup>. Samples were homogenized and normalized to 0.125 µg/µL protein (BCA protein assay, Pierce, Rockford, IL, USA) in a 2X SDS-PAGE sample buffer. Samples were boiled for 2 minutes and then stored at –80°C. Protein was further diluted 1:15 in 1X sample buffer before loading 10 µL of each sample into each lane. Two additional lanes were loaded with homogenized adult rat soleus muscle standard, which contains the four adult skeletal muscle myosin isoforms (types I, IIa, IIb and IIx)<sup>30; 31</sup>. Total acrylamide concentration was 4% and 8% in the stacking and resolving gels, respectively (bisacrylamide, 1:50). Gels (16 cm × 22 cm × 0.75 mm thick) were run at a constant current of 10 mA for 1 h, followed by a constant voltage of 275 V for 22 h at 4°C. Gels were silver stained according to the Silver Stain Plus procedure (BioRad, Hercules, CA). MHC sample bands were identified by comparing position against the rat standard. Relative band intensity was quantified (GS-800, BioRad) and used to compute percent composition of each MHC isoform.

## Histology

To evaluate muscle fiber cross-sectional area (CSA) and the percentage of centralized nuclei (CN) as measures of atrophy and regeneration, respectively, sections were stained with wheat germ agglutinin (Invitrogen, Alexa Fluor 594, 1:2000) and coverslipped with mounting medium with 4',6-diamidino-2-phenylindole (Vectashield Antifade mounting medium with DAPI, VectorLabs). CSA and CN were then quantified using a custom ImageJ macro<sup>32</sup>. The frequency of muscle fiber degeneration was quantified by overlaying a 500 $\mu\text{m}^2$  grid over an entire Hematoxylin and Eosin-stained (H & E) section and scoring each grid element as either positive or negative for signs of muscle fiber degeneration. Signs of muscle degeneration were defined as: hypercellularity (i.e. myophagocytic fibers with multiple non-peripheral nuclei), disrupted muscle fiber membranes, or split muscle fibers<sup>18</sup>.

Fat accumulation was quantified using two methods, one to approximate total fat content, and a second to determine the localization of fat relative to fascicular structures. The overall fat fraction of each region was quantified as the percentage of the entire muscle segment staining positive for Oil Red-O, as determined by a semi-automated thresholding protocol (Metamorph). Localization of fat was quantified using a similar strategy as used to quantify muscle fiber degeneration, reported as a percentage of grid elements containing either intra-fascicular or peri-fascicular fat. As a potential marker of more 'terminal' degeneration, the incidence of intra-fascicular fat adjacent to degenerating muscle fibers (i.e. contained within the same grid element) was determined. Fibrosis was quantified using a bulk tissue, hydroxyproline assay as well as histology. Hydroxyproline content was calculated and converted to bulk collagen content using established methods<sup>37</sup> while a semi-automated thresholding algorithm was used to quantify the percentage of each muscle section occupied by connective tissue as determined by Gomori trichrome staining.

## Statistical Analysis

Architectural changes immediately after tenotomy (n=5 animals) were first compared across regions between tenotomy and the unoperated contralateral side using two-way, repeated measures analyses of variance (ANOVA). To examine the effects of time  $\times$  treatment (tenotomy versus sham surgery) on each histological parameter, each region was analyzed individually using two-way ANOVA. Multiple comparisons were performed between timepoints using Sidak's post-hoc testing.

Additionally, for simplicity and in order to compare these data to previously published work (where information on the muscle region evaluated is often omitted), the mean of all four regions is reported as the "whole muscle" average for each parameter. In the immediate architecture group, the mean "whole muscle" data was compared between tenotomy and contralateral using t-tests. For the time series animals (n=6 per time point), the mean "whole muscle" data was analyzed for time  $\times$  treatment using two-way ANOVA. Analysis was performed in GraphPad Prism version 8 with level of significance set  $\alpha = 0.05$ .

## Results

In the 5 animals sacrificed immediately following tenotomy, architectural changes confirmed a robust mechanical unloading of the supraspinatus muscle as the total muscle length was significantly retracted to an average distance of 7.3 millimeters ( $p = 0.0006$ ) (Fig 1A). Fiber length also decreased significantly ( $p = 0.0016$ ) (Fig 1B). Significant sarcomere shortening was also observed with tenotomy, as expected, with a mean shortening of 0.45 microns ( $p = 0.0011$ ) (Fig 1C). Pennation angle showed no differences between sham and tenotomy within one region, although differences between regions were observed (Fig 1D).

In the time series group ( $n = 30$  rabbits), retraction distance increased over time to a maximum mean retraction of 14.5 mm at 16 weeks, with statistically significant changes beginning at 4 weeks (effect of time,  $p < 0.0001$ ) (Fig 2A). By 2 weeks post-tenotomy, muscle mass was significantly reduced compared to the sham side, with persistent mass reduction of 25% at 16 weeks (effect of treatment,  $p < 0.0001$ ) (Fig 2B). Muscle mass also decreased over time from week 1 to weeks 4 and 8 (effect of time,  $p = 0.0063$ ; interaction,  $p = 0.0238$ ). Muscle fiber cross-sectional area was significantly decreased at 4 and 16 weeks post-tenotomy, measuring 26.5% smaller than the contralateral side at 16 weeks (effect of treatment,  $p < 0.0001$ ) (Fig 2C).

The myosin heavy chain isoform profile of the supraspinatus in the timeseries data showed a significant effect of treatment in decreasing the MHC type I slow isoform content ( $p = 0.0246$ ) (Fig 3, Supp Fig 1A). There was a corresponding increase in the MHC type IIa fast oxidative isoform as well as the MHC type IIb and IIx fast glycolytic isoforms (Supp Fig 1B–D). These changes showed significant effects of treatment for each isoform ( $p = 0.0281$  for IIa;  $p = 0.0336$  for IIb;  $p = 0.0166$  for IIx). Type IIa and type IIb MHC increased significantly as an effect of time ( $p = 0.0003$  and  $p = 0.0006$ , respectively) as well.

Muscle degeneration was significantly increased with tenotomy compared to sham surgery ( $p = 0.0006$ ), but there was no significant effect of time (Fig 4A–B). The percentage of regions demonstrating signs of degeneration remained below 1% on the control side, excluding the 1-week timepoint, while ranging from approximately 1–3% in the post-tenotomy specimens. Additionally, there was no increase in regeneration—as measured by the percentage of centralized nuclei—in the tenotomized muscle compared to the contralateral side (Fig 4C–D), though there was a significant effect of time ( $p = 0.0008$ ).

Along with muscular changes, fat and fibrosis are key characteristics of RC muscle pathology. There was an increase in collagen content in the tenotomized shoulders that appeared at 4 weeks and persisted through 16 weeks (effect of treatment,  $p = 0.0010$ ; effect of time,  $p = 0.0048$ ; interaction,  $p = n.s.$ ) (Fig 5A). The highest collagen content was observed at 4 weeks post-tenotomy with mean 16  $\mu\text{g}$  collagen / mg tissue, while the largest difference in fibrosis occurred at 8 weeks. Overall fat accumulation, as measured by whole-cross section Oil Red-O staining, was significantly higher at 16 weeks post-tenotomy compared to sham or any other tenotomy time point except 4 weeks (effect of treatment,  $p < 0.0001$ ; effect of time,  $p = 0.0007$ ; interaction,  $p = 0.0031$ ) (Fig 5B). At 16 weeks,

fat content comprised 7.4% of CSA, nearly tripled compared to 2.5% in the contralateral control.

In terms of localization, fat was more often found between fascicles (inter-fascicular) than within fascicles (intra-fascicular) in both the tenotomized and contralateral muscle (Fig 6A). Inter-fascicular fat was seen in 35% of regions one week after tenotomy versus 23% contralaterally, which gradually decreased to 25% versus 16% at 16 weeks (tenotomy and contralateral, respectively) (Fig 6B). Tenotomy significantly increased the proportion of inter-fascicular fat compared to sham surgery (effect of treatment,  $p < 0.0001$ ; effect of time,  $p = 0.0108$ ; interaction,  $p = \text{n.s.}$ ), with the 1-week time point showing a significant difference between treatments. In contrast, the incidence of intra-fascicular fat was significantly increased by tenotomy at 1, 4, and 16 weeks post-tenotomy (all  $p < 0.05$ ) (Fig 6C). The percentage of regions demonstrating intra-fascicular fat remained below 3% in the sham surgery group but ranged from 9–16% in the post-tenotomy shoulders (effect of treatment,  $p < 0.0001$ ). Fat localization was then further analyzed for the appearance of intra-fascicular fat contained within the same grid element as degenerating muscle fibers, as a potential marker terminal degeneration. While there was virtually no incidence of intra-fascicular fat adjacent to degenerating muscle fibers in contralateral muscles, tenotomized muscles showed a significant increase in this feature (effect of treatment,  $p < 0.0001$ ; effect of time,  $p = 0.0102$ ; interaction,  $p = \text{n.s.}$ ). The highest proportion of affected regions was observed at 16 weeks, accounting for 3.0% of post-tenotomy regions and 0.6% on the sham side ( $p = 0.0123$ ).

## Discussion

The present study is the first, to our knowledge, to demonstrate increased muscle degeneration in a rabbit tenotomy model as a separate and distinct finding from muscle atrophy. It is also the first to quantify immediate architectural changes, lack of muscle regeneration, and the shift from slow to fast myosin heavy chain isoforms in the tenotomized supraspinatus over time. These muscle changes are accompanied by two other key clinical markers of disease progression: significant and progressive fatty infiltration, and apparent fibrosis. Finally, though the incidence is lower than in chronic human tears, a progressive increase in degenerating muscle fibers adjacent to intra-fascicular fat was observed. This is another previously undescribed finding. These results show that the rabbit supraspinatus is a clinically relevant, cost-effective animal model of RC disease. Furthermore, findings of muscle atrophy and fat accumulation are consistently reproducible across different teams of investigators, and the current study expands upon a well-delineated timeline of tissue changes for evaluating future interventions.

Immediately after tenotomy, muscle length, fiber length, and sarcomere length were all significantly reduced compared to the unoperated side. These are not unexpected findings but serve to establish the extent to which the muscle releases from surrounding soft tissue structures, retracts, and mechanically unloads. Importantly, the tenotomized supraspinatus muscle also continued to retract over the time course investigated here. This suggests that the muscle does not scar down and become reloaded with the effective use of a Penrose drain in this model.



Tenotomy produced early radial muscle atrophy, as measured by muscle mass and fiber cross-sectional area loss, which went on to be stable over the 16-week time course. The lack of statistical differences in muscle fiber CSA noted at 8 weeks can be explained by fluctuations on the sham side rather than variation in the tenotomized muscle response, but the source of these changes on the control side are elusive despite re-sampling. One possible explanation for the decrease in CSA at 1–2 weeks on the right side is post-surgical changes from the sham operation, suggesting a potential benefit of using an unoperated control. The early timing of radial atrophy did correspond with macroscopic changes at 2 and 4 weeks in muscle mass and retraction, respectively. These findings are similar to the previous literature, but prior studies used 6 weeks as the earliest timepoint<sup>9; 10</sup>. However, a recent study by Abdou et al<sup>27</sup> that graded the degree of muscle atrophy by histological characteristics (angular versus round muscle fiber shape, decreased fiber size, and decreased distance between myonuclei and centralized myonuclei) found that atrophy increases from mild-to-moderate at 2 and 4 weeks to moderate by 6 weeks. At 8 and 12 weeks, the mean grade of muscle atrophy was closer to their definition of severe, advanced disease. The advantage here is that the atrophy is quantified. In humans, muscle atrophy following RC tear<sup>25; 33</sup> likely happens more gradually due to an insidious onset and progression of tendon tear<sup>34</sup>, but the course of these changes is important to understand with high time-resolution in a preclinical model of disease.

Another parallel to human patients was the MHC isoform composition, which has not been studied before in the rabbit supraspinatus tenotomy model. When all isoforms are considered separately, human supraspinatus muscle contains the most type I MHC fibers, previously estimated as 36.72%<sup>35</sup> and 54%<sup>36</sup> using different techniques and mean cadaver ages (76.1<sup>35</sup> and 65±12<sup>36</sup> years, respectively). However, when combined, the fast type II isoforms comprise the majority, reflecting the muscle's role in active shoulder motion as well. Patients undergoing arthroscopy with full-thickness RC tears possess significantly lower type I MHC content compared to partial-thickness tears, but similar amounts of type II MHC and smaller fiber sizes of both<sup>33</sup>. Similarly, supraspinatus tenotomy in these rabbits led to a shift from slow type I MHC isoforms to fast type IIb and IIx MHC isoforms as a significant effect of treatment and time. This potentially reflects tear-induced weakening/disuse of slow muscle fiber functions such as glenohumeral stabilization or resistance to fatigue. In contrast, a rabbit RC model using the subscapularis muscle found no difference in MHC isoform composition after partial or complete tear creation, nor after denervation<sup>37</sup>. Furthermore, intact rat RC muscles are composed of <10% type I MHC, emphasizing that the shoulder musculature in this rodent model has a nearly completely fast twitch functionality that differs from human subjects<sup>38</sup>.

Our evolving understanding of human RC pathophysiology also prompted investigation of muscle degeneration as a separate finding from muscle atrophy. Whereas atrophy induced by unloading or inactivity can be nearly reversible with reloading<sup>39–42</sup>, muscle degeneration in the context of chronic human RC disease is a process of irreversible muscle damage and cell death<sup>18; 19</sup>. Similarly, this rabbit model showed a significant increase in muscle degeneration after tenotomy, as well as degeneration adjacent to intra-fascicular fat. The latter finding has been used as a measure of advanced disease in humans, where it may indicate irreversibly degenerated muscle fibers and an area of existing or impending terminal

“fatty replacement”<sup>18</sup>. The present study is the first to report this phenomenon in the rabbit RC, further demonstrating the suitability of this model to address questions of mechanism or adjuvant therapy. Future directions could include extracting transcriptional or proteomic data from the rabbit model in lieu of human samples, with correlation to the timeline of tissue changes described here. The current study also found no difference in muscle regeneration after tenotomy versus sham surgery. From a model perspective, this is not necessarily detrimental, as diminished regenerative capacity is thought to be a feature of irreversible muscle loss in humans<sup>19; 33</sup>. Again, these are important structural changes to investigate over time, serving as reference points for more in-depth transcriptional study in the future.

Beyond muscle loss, the development of fatty infiltration and fibrosis are important from a clinical perspective. Not only is fat accumulation a potential contributor to the irreversibility of muscle loss<sup>18; 19</sup>, it is also an important clinical diagnostic feature<sup>43; 44</sup>. Existing mouse and rat models have demonstrated minimal fatty infiltration, unless combined with nerve transection or in cases of nerve transection alone<sup>7; 8</sup>. In rabbits, however, the present study confirms a recent finding by Valencia et al<sup>24</sup> that a preponderance of fat accumulation occurs in the inter-fascicular space. Yet the presence of intra-fascicular fat, especially alongside degenerating muscle fibers, may represent a more biologically significant fat depot. Compared to other studies, the current investigation examined fat accumulation at earlier and more frequent time points. Inter-fascicular fat was significantly increased as early as one week after tenotomy, while intra-fascicular fat content fluctuated with peaks at 1, 4, and 16 weeks. Interestingly, this pattern is the inverse of inflammatory cell infiltration, which appears to have bimodal peaks at 2 and 6–8 weeks in this model<sup>27</sup>. Overall, inter- or intra-fascicular fat quantification appears to be more sensitive to early changes than fat percentage of CSA, which did not reach a statistically significant increase within time point groups until 16 weeks. Collagen content, as a metric of fibrosis, also showed a modest increase beginning at four weeks. However, as the hydroxyproline assay determines collagen on a per-weight basis, it is unclear to what degree this result is a function of *de novo* collagen synthesis versus a relative increase due to a reduction in muscle content. In future experiments, fraction synthetic rates of collagen should be examined.

On the basis of the data presented here and in other recent work<sup>9</sup>, the rabbit is a strong preclinical model for both basic science and translational research related to RC disease. However, there are some notable limitations to the present study. In the time course studied here, there was a low incidence of muscle degeneration and no signs of regeneration compared to late-stage disease in humans<sup>18</sup>. The present construct and time frame may be less well-suited for modelling a chronic tear with near-complete loss of muscle and replacement by fat/connective tissue, without allowing for a longer period of muscle retraction and degeneration. Yet this should not preclude the rabbit from being used as a suitable model for the intermediate stages of RC disease that are clinically relevant to target and treat. Additionally, performing a sham surgery on the control shoulder may have led to a smaller effect size than using a native unoperated shoulder as the control.

The challenges of studying RC disease in humans necessitate an animal model that faithfully recapitulates the muscle phenotype found in humans. In this study, we demonstrate that tenotomy leads to significant acute muscle retraction which progresses through 16

weeks. Similar to human RC, both atrophic and degenerative mechanisms of muscle loss are present in the rabbit following RC tear. Furthermore, fat accumulates in both inter- and intra-fascicular spaces, suggesting that the rabbit is a suitable model for studying both bulk fatty infiltration as well as the potentially more terminal process of fat replacing muscle fibers within the fascicular structure. On this basis, we believe the rabbit is an appropriate preclinical model for studying biological questions as well as evaluating new regenerative therapies aimed toward restoring RC function.

## Supplementary Material

Refer to Web version on PubMed Central for supplementary material.

## Acknowledgements

This study was partially supported by NIH R21AR072523, and partially by unrestricted internal funds. The authors have no financial conflicts of interest related to the work presented in this manuscript.

## References

1. Yamamoto A, Takagishi K, Osawa T, et al. 2010. Prevalence and risk factors of a rotator cuff tear in the general population. *J Shoulder Elbow Surg* 19:116–120. [PubMed: 19540777]
2. MacDermid JC, Ramos J, Drosdowech D, et al. 2004. The impact of rotator cuff pathology on isometric and isokinetic strength, function, and quality of life. *J Shoulder Elbow Surg* 13:593–598. [PubMed: 15570226]
3. Galatz LM, Ball CM, Teefey SA, et al. 2004. The outcome and repair integrity of completely arthroscopically repaired large and massive rotator cuff tears. *J Bone Joint Surg Am* 86:219–224. [PubMed: 14960664]
4. Deniz G, Kose O, Tugay A, et al. 2014. Fatty degeneration and atrophy of the rotator cuff muscles after arthroscopic repair: does it improve, halt or deteriorate? *Arch Orthop Trauma Surg* 134:985–990. [PubMed: 24845686]
5. Gladstone JN, Bishop JY, Lo IK, et al. 2007. Fatty infiltration and atrophy of the rotator cuff do not improve after rotator cuff repair and correlate with poor functional outcome. *Am J Sports Med* 35:719–728. [PubMed: 17337727]
6. Kim HM, Galatz LM, Lim C, et al. 2012. The effect of tear size and nerve injury on rotator cuff muscle fatty degeneration in a rodent animal model. *J Shoulder Elbow Surg* 21:847–858. [PubMed: 21831663]
7. Liu X, Laron D, Natsuhara K, et al. 2012. A mouse model of massive rotator cuff tears. *J Bone Joint Surg Am* 94:e41. [PubMed: 22488625]
8. Liu X, Manzano G, Kim HT, et al. 2011. A rat model of massive rotator cuff tears. *J Orthop Res* 29:588–595. [PubMed: 20949443]
9. Farshad M, Meyer DC, Nuss KM, et al. 2012. A modified rabbit model for rotator cuff tendon tears: functional, histological and radiological characteristics of the supraspinatus muscle. *Shoulder & Elbow* 4:90–94.
10. Rubino LJ, Stills HF Jr, Sprott DC, et al. 2007. Fatty infiltration of the torn rotator cuff worsens over time in a rabbit model. *Arthroscopy* 23:717–722. [PubMed: 17637406]
11. Gerber C, Meyer DC, Schneeberger AG, et al. 2004. Effect of tendon release and delayed repair on the structure of the muscles of the rotator cuff: an experimental study in sheep. *J Bone Joint Surg Am* 86:1973–1982. [PubMed: 15342760]
12. Luan T, Liu X, Easley JT, et al. 2015. Muscle atrophy and fatty infiltration after an acute rotator cuff repair in a sheep model. *Muscles, ligaments and tendons journal* 5:106.

13. Gerber C, Meyer DC, Flück M, et al. 2015. Anabolic steroids reduce muscle degeneration associated with rotator cuff tendon release in sheep. *Am J Sports Med* 43:2393–2400. [PubMed: 26304962]
14. Oh JH, Chung SW, Kim SH, et al. 2014. 2013 Neer Award: Effect of the adipose-derived stem cell for the improvement of fatty degeneration and rotator cuff healing in rabbit model. *J Shoulder Elbow Surg* 23:445–455. [PubMed: 24129058]
15. Davies MR, Liu X, Lee L, et al. 2016. TGF-beta Small Molecule Inhibitor SB431542 Reduces Rotator Cuff Muscle Fibrosis and Fatty Infiltration By Promoting Fibro/Adipogenic Progenitor Apoptosis. *PLoS One* 11:e0155486. [PubMed: 27186977]
16. Gerber C, Meyer DC, Nuss KM, et al. 2011. Anabolic steroids reduce muscle damage caused by rotator cuff tendon release in an experimental study in rabbits. *J Bone Joint Surg Am* 93:2189–2195. [PubMed: 22159854]
17. Gerber C, Meyer DC, Frey E, et al. 2009. Neer Award 2007: Reversion of structural muscle changes caused by chronic rotator cuff tears using continuous musculotendinous traction. An experimental study in sheep. *J Shoulder Elbow Surg* 18:163–171. [PubMed: 19095462]
18. Gibbons MC, Singh A, Anakwenze O, et al. 2017. Histological Evidence of Muscle Degeneration in Advanced Human Rotator Cuff Disease. *J Bone Joint Surg Am* 99:190–199. [PubMed: 28145949]
19. Gibbons MC, Singh A, Engler AJ, et al. 2018. The role of mechanobiology in progression of rotator cuff muscle atrophy and degeneration. *J Orthop Res* 36:546–556. [PubMed: 28755470]
20. Mendias CL, Roche SM, Harning JA, et al. 2015. Reduced muscle fiber force production and disrupted myofibril architecture in patients with chronic rotator cuff tears. *J Shoulder Elbow Surg* 24:111–119. [PubMed: 25193488]
21. Gerber C, Meyer DC, Flück M, et al. 2016. Muscle Degeneration Associated With Rotator Cuff Tendon Release and/or Denervation in Sheep. *Am J Sports Med*:0363546516677254.
22. Trudel G, Ryan SE, Rakhra K, et al. 2010. Extra- and intramuscular fat accumulation early after rabbit supraspinatus tendon division: depiction with CT. *Radiology* 255:434–441. [PubMed: 20413756]
23. Fabis J, Kordek P, Bogucki A, et al. 1998. Function of the rabbit supraspinatus muscle after detachment of its tendon from the greater tubercle: Observations up to 6 months. *Acta orthopaedica Scandinavica* 69:570–574. [PubMed: 9930099]
24. Valencia AP, Lai JK, Iyer SR, et al. 2018. Fatty Infiltration Is a Prognostic Marker of Muscle Function After Rotator Cuff Tear. *Am J Sports Med* 46:2161–2169. [PubMed: 29750541]
25. Steinbacher P, Tauber M, Kogler S, et al. 2010. Effects of rotator cuff ruptures on the cellular and intracellular composition of the human supraspinatus muscle. *Tissue and Cell* 42:37–41. [PubMed: 19709709]
26. Fabis J, Kordek P, Bogucki A, et al. 2000. Function of the rabbit supraspinatus muscle after large detachment of its tendon: 6-week, 3-month, and 6-month observation. *J Shoulder Elbow Surg* 9:211–216. [PubMed: 10888165]
27. Abdou MA, Kim GE, Kim J, et al. 2019. How Long Should We Wait to Create the Goutallier Stage 2 Fatty Infiltrations in the Rabbit Shoulder for Repairable Rotator Cuff Tear Model? *Biomed Res Int* 2019:7387131. [PubMed: 31061826]
28. Lieber RL, Yeh Y, Baskin RJ. 1984. Sarcomere length determination using laser diffraction. Effect of beam and fiber diameter. *Biophysical journal* 45:1007. [PubMed: 6610443]
29. Talmadge RJ, Roy RR. 1993. Electrophoretic separation of rat skeletal muscle myosin heavy-chain isoforms. *J Appl Physiol* (1985) 75:2337–2340. [PubMed: 8307894]
30. Schiaffino S, Gorza L, Sartore S, et al. 1989. Three myosin heavy chain isoforms in type 2 skeletal muscle fibres. *J Muscle Res Cell Motil* 10:197–205. [PubMed: 2547831]
31. Schiaffino S, Reggiani C. 1994. Myosin isoforms in mammalian skeletal muscle. *J Appl Physiol* (1985) 77:493–501. [PubMed: 8002492]
32. Minamoto VB, Hulst JB, Lim M, et al. 2007. Increased efficacy and decreased systemic-effects of botulinum toxin A injection after active or passive muscle manipulation. *Developmental Medicine & Child Neurology* 49:907–914. [PubMed: 18039237]

33. Lundgreen K, Lian ØB, Engebretsen L, et al. 2013. Lower muscle regenerative potential in full-thickness supraspinatus tears compared to partial-thickness tears. *Acta orthopaedica* 84:565–570. [PubMed: 24171689]
34. Bigliani LU, Cordasco FA, McIlveen SJ, et al. 1992. Operative repair of massive rotator cuff tears: long-term results. *J Shoulder Elbow Surg* 1:120–130. [PubMed: 22971604]
35. Potau JM, Artells R, Munoz C, et al. 2012. Expression of myosin heavy chain isoforms in the human supraspinatus muscle: variations related to age and sex. *Cells Tissues Organs* 196:456–462. [PubMed: 22699393]
36. Lovering RM, Russ DW. 2008. Fiber type composition of cadaveric human rotator cuff muscles. *J Orthop Sports Phys Ther* 38:674–680. [PubMed: 18978449]
37. Rowshan K, Hadley S, Pham K, et al. 2010. Development of fatty atrophy after neurologic and rotator cuff injuries in an animal model of rotator cuff pathology. *J Bone Joint Surg Am* 92:2270–2278. [PubMed: 20926720]
38. Rui Y, Pan F, Mi J. 2016. Composition of Muscle Fiber Types in Rat Rotator Cuff Muscles. *Anat Rec (Hoboken)* 299:1397–1401. [PubMed: 27314819]
39. Frontera WR, Meredith CN, O'reilly K, et al. 1988. Strength conditioning in older men: skeletal muscle hypertrophy and improved function. *Journal of applied physiology* 64:1038–1044. [PubMed: 3366726]
40. Jones SW, Hill RJ, Krasney PA, et al. 2004. Disuse atrophy and exercise rehabilitation in humans profoundly affects the expression of genes associated with the regulation of skeletal muscle mass. *The FASEB journal* 18:1025–1027. [PubMed: 15084522]
41. Raue U, Slivka D, Jemiolo B, et al. 2006. Myogenic gene expression at rest and after a bout of resistance exercise in young (18–30 yr) and old (80–89 yr) women. *Journal of Applied Physiology* 101:53–59. [PubMed: 16601301]
42. Schoenfeld BJ. 2012. Does exercise-induced muscle damage play a role in skeletal muscle hypertrophy? *The Journal of Strength & Conditioning Research* 26:1441–1453. [PubMed: 22344059]
43. Goutallier D, Postel J-M, Bernageau J, et al. 1994. Fatty muscle degeneration in cuff ruptures: pre- and postoperative evaluation by CT scan. *Clin Orthop Relat Res* 304:78–83.
44. Goutallier D, Postel J-M, Gleyze P, et al. 2003. Influence of cuff muscle fatty degeneration on anatomic and functional outcomes after simple suture of full-thickness tears. *J Shoulder Elbow Surg* 12:550–554. [PubMed: 14671517]

**Statement of Clinical Relevance:**

Rabbit supraspinatus tenotomy recapitulates key features of the pathophysiology of human RC tears, including muscle atrophy and degeneration, lack of regeneration, fat accumulation, and fibrosis.

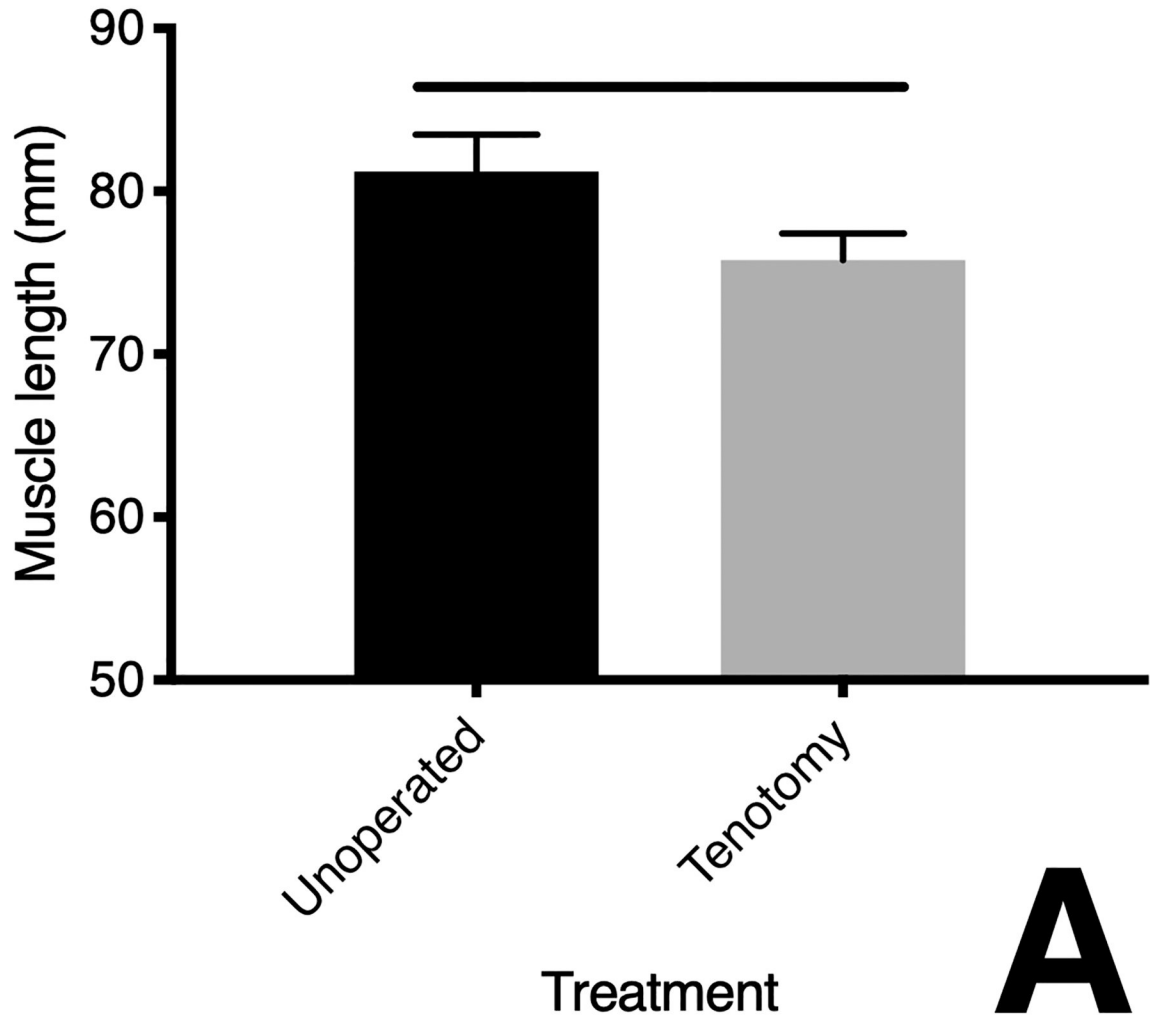
Author Manuscript

Author Manuscript

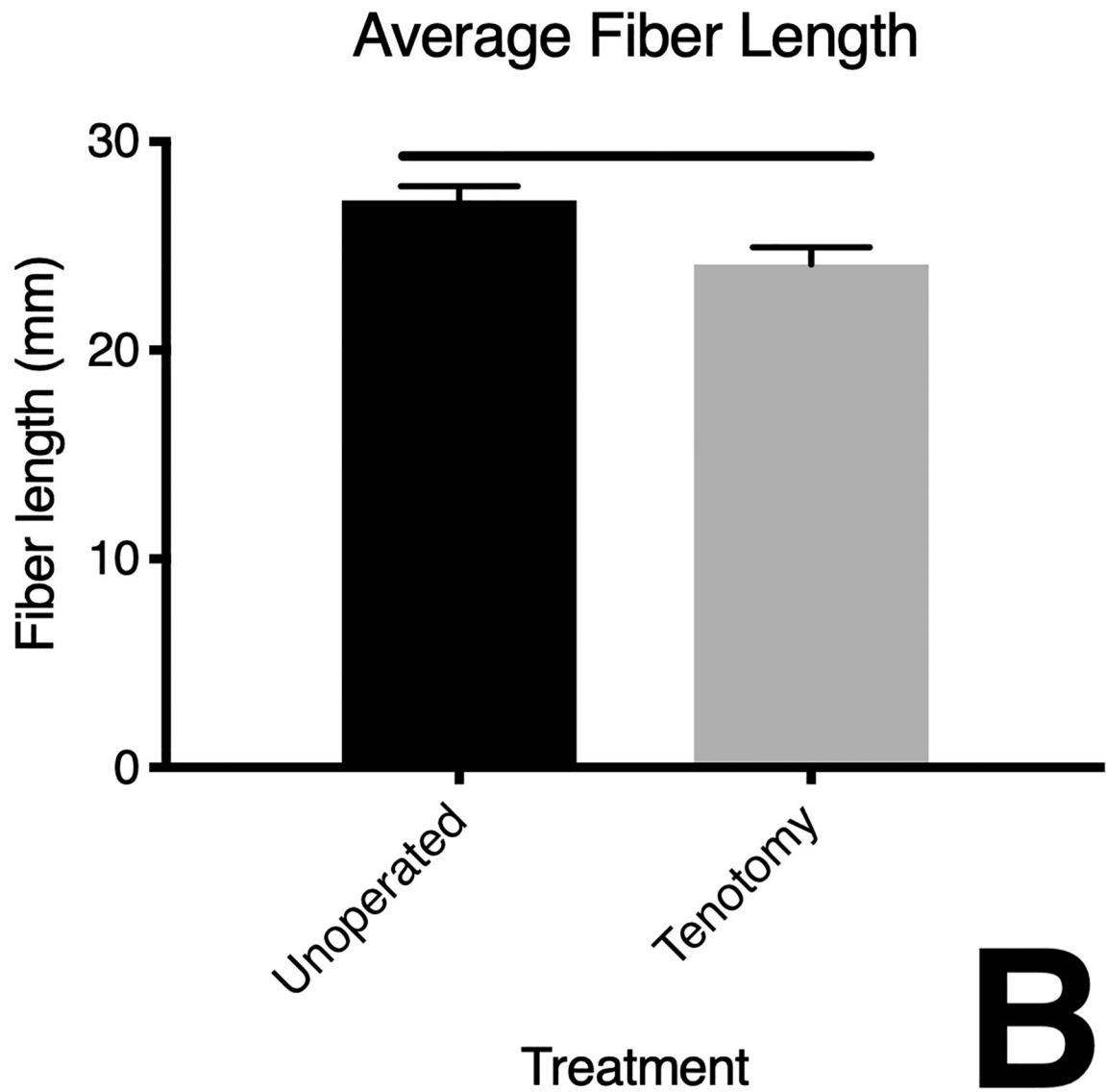
Author Manuscript

Author Manuscript

# Average Muscle Length

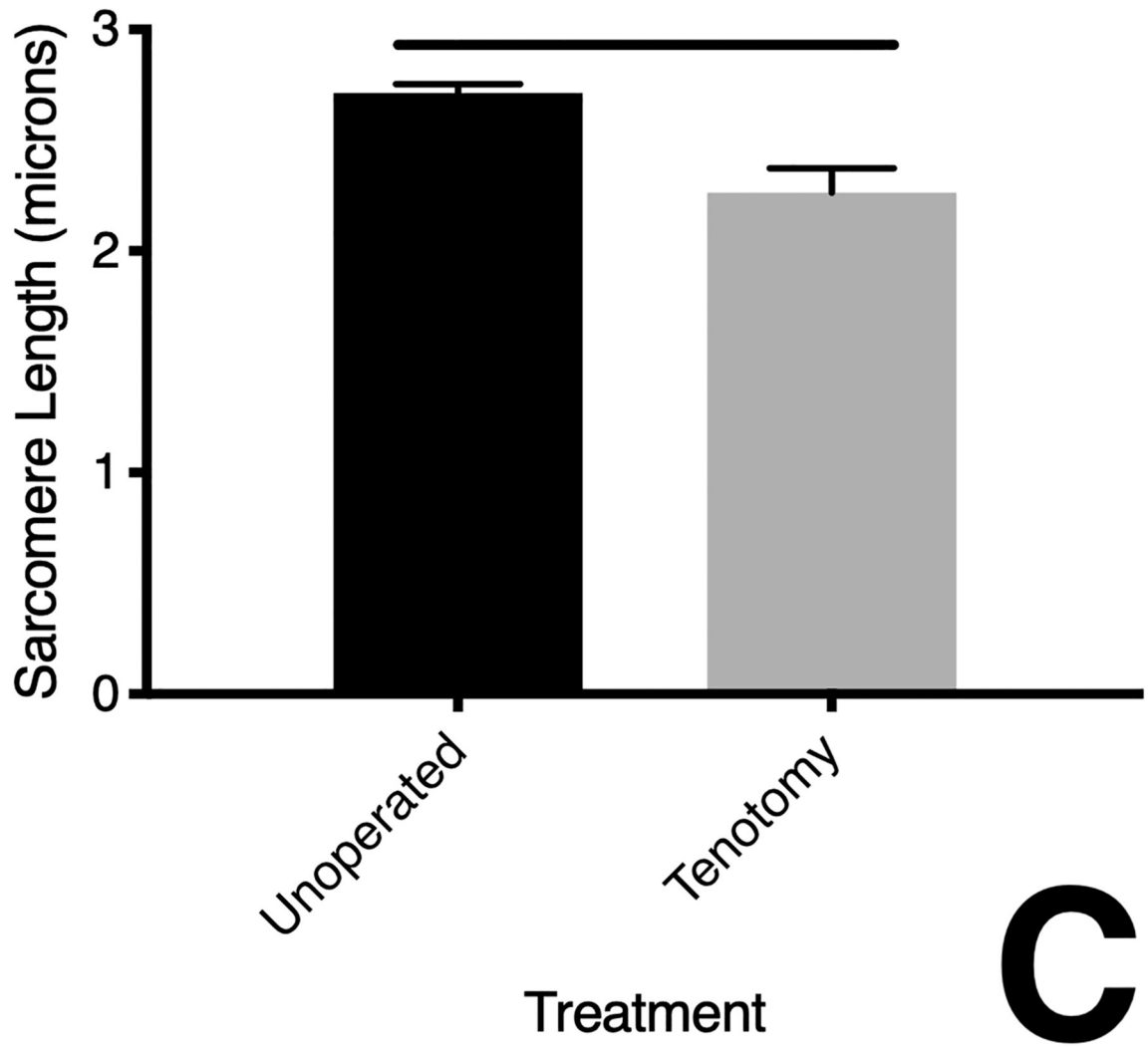


# A





# Average Sarcomere Length



Author Manuscript

Author Manuscript

Author Manuscript

Author Manuscript

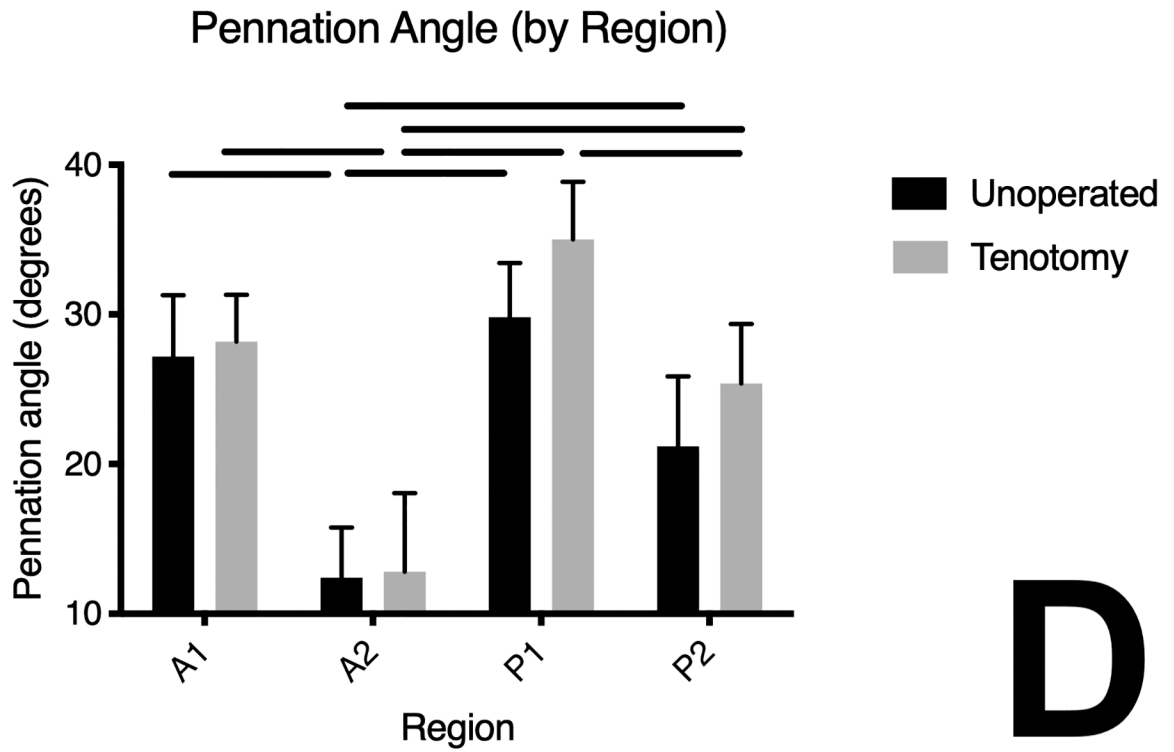
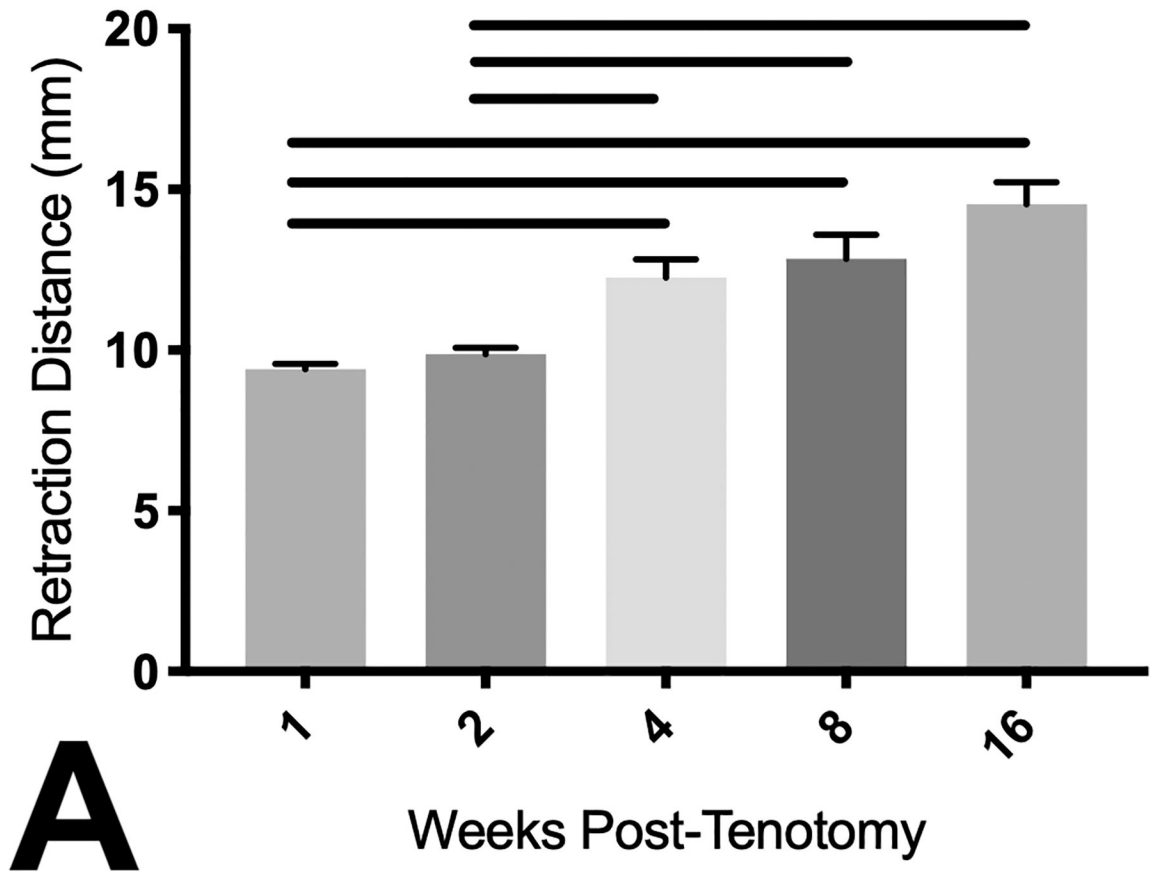


**Fig 1.** Changes in muscle architecture immediately following supraspinatus tenotomy in rabbits (n=5). Comparison of muscle length (Fig 1A), fiber length (Fig 1B), sarcomere length (Fig 1C), and pennation angle by region (Fig 1D) to the unoperated contralateral side. Means with standard error shown; horizontal bar denotes  $p < 0.05$  within time point or within treatment group.

# Retraction Distance

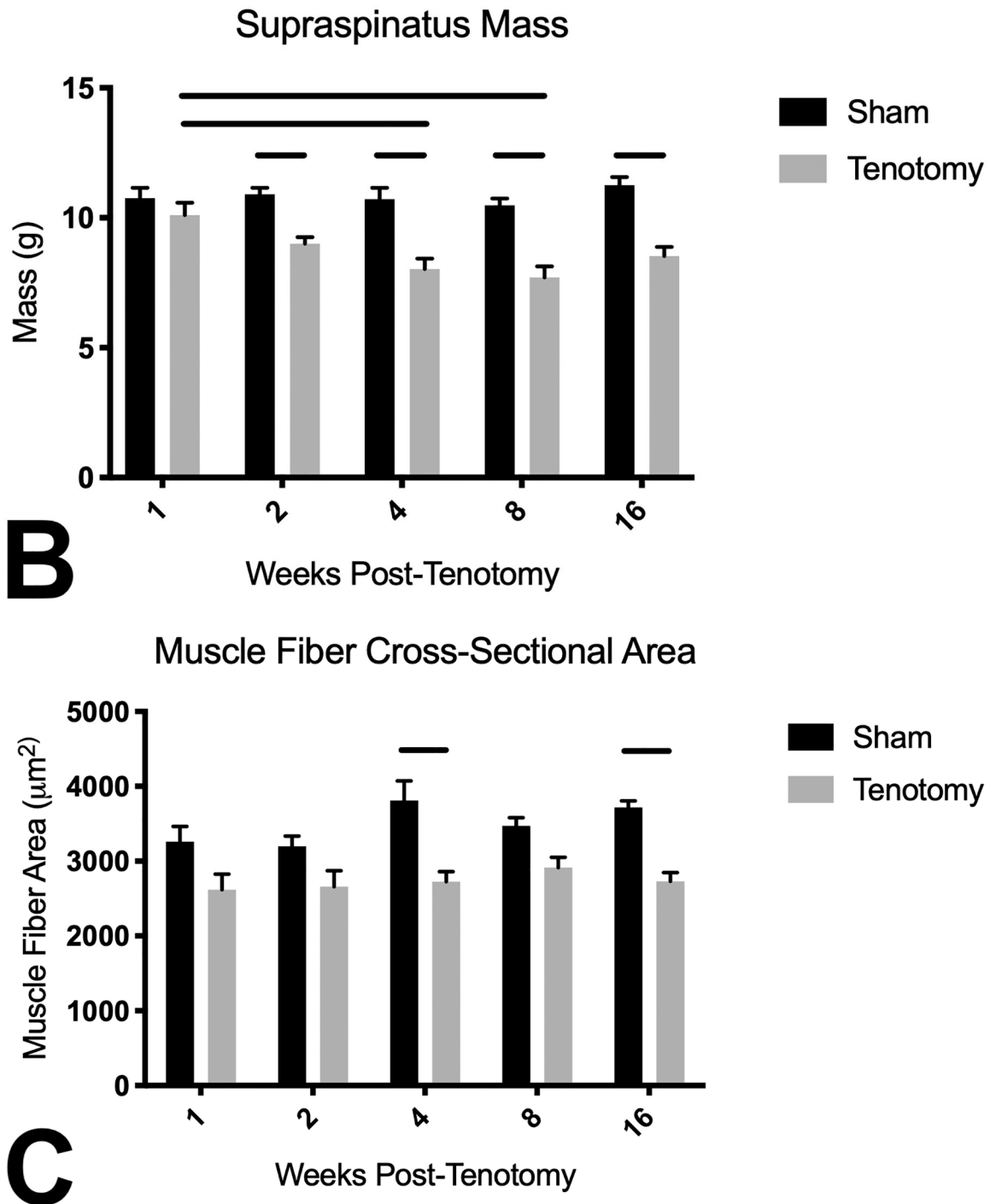


Author Manuscript

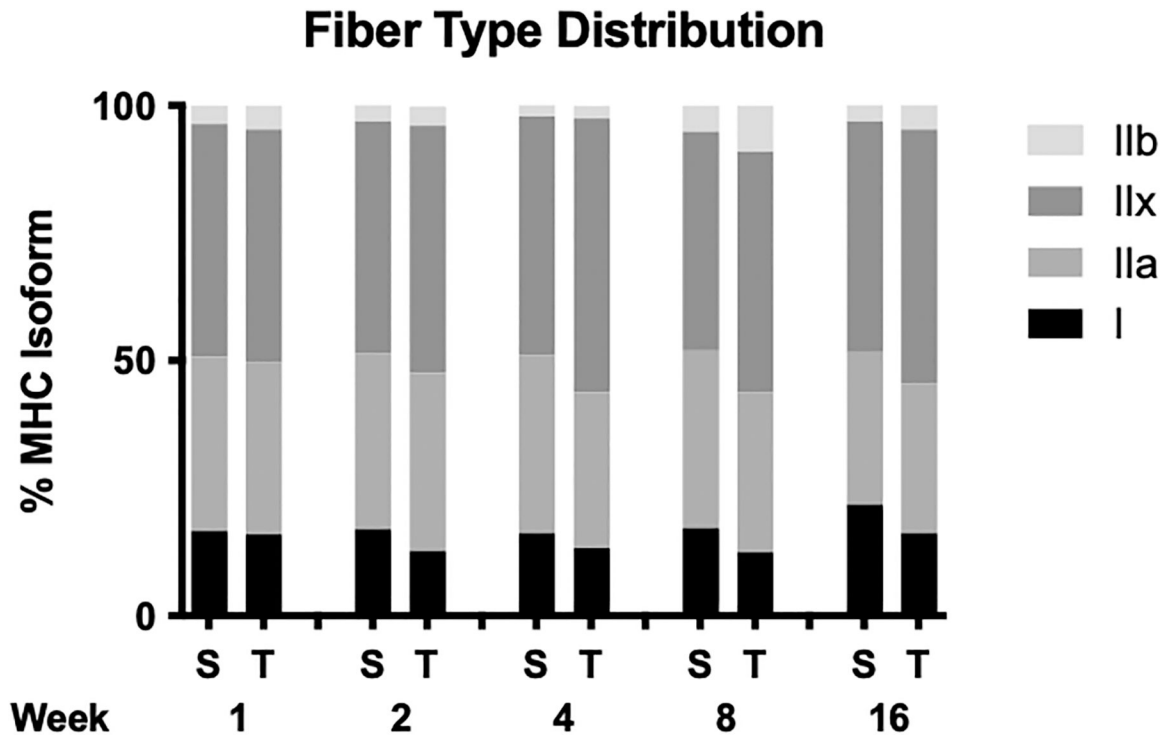
Author Manuscript

Author Manuscript

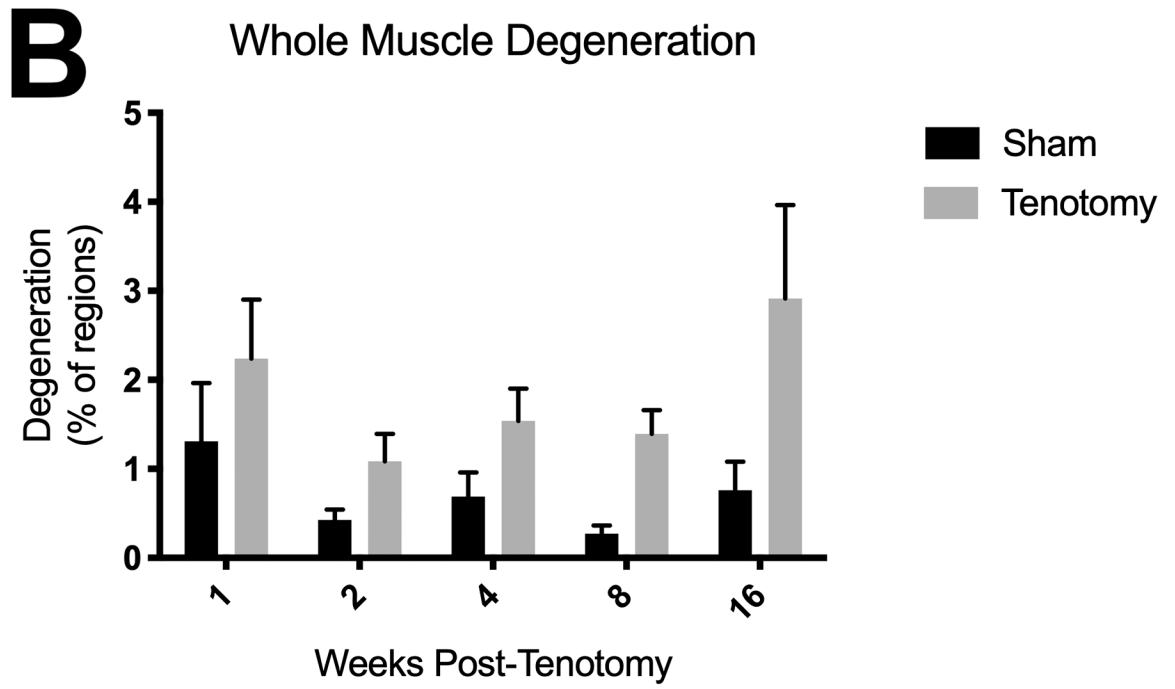
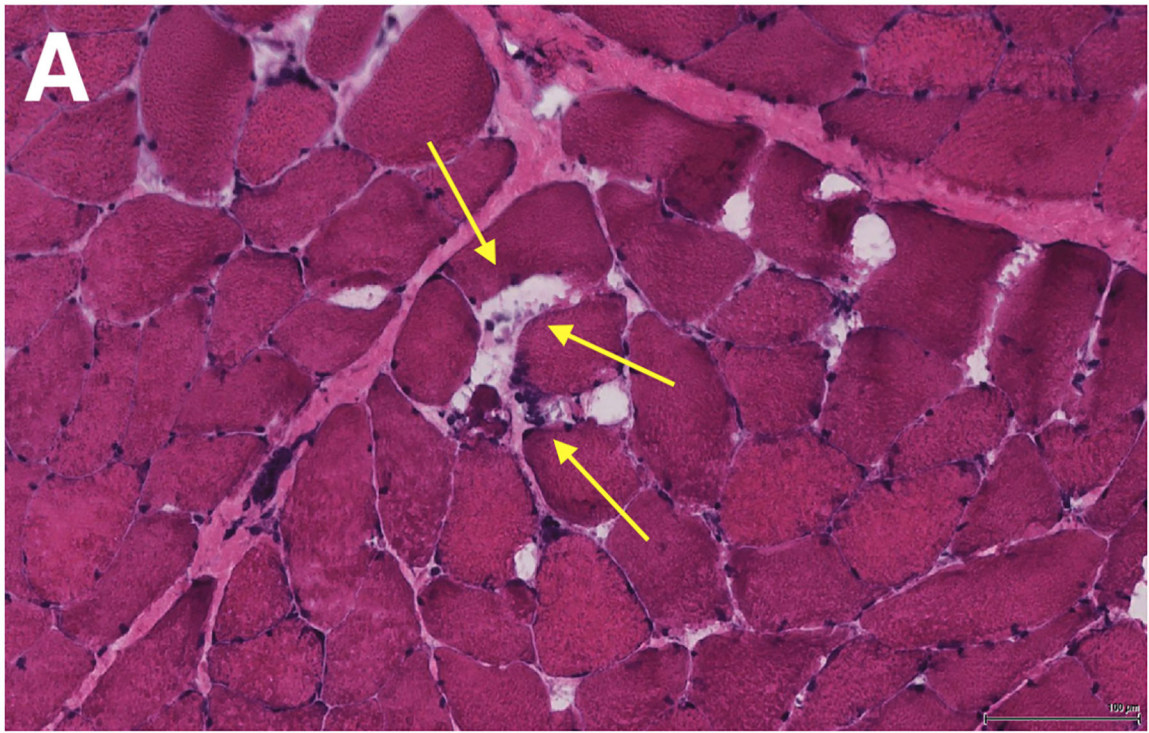
Author Manuscript

**Fig 2.**

Post-tenotomy changes over time in supraspinatus retraction distance (Fig 2A). Comparison of post-tenotomy muscle mass (Fig 2B) and fiber cross-sectional area (Fig 2C) to sham surgery on the contralateral side. N=6 rabbits at each time point. Means with standard error shown; horizontal bar denotes  $p < 0.05$  within time point or within treatment group.



**Fig 3.** Distribution of myosin heavy chain (MHC) isoforms over time after tenotomy versus contralateral sham surgery in the whole muscle. S, sham; T, tenotomy. Means shown; horizontal bar denotes  $p < 0.05$  within time point or within treatment group. Error bars excluded for visual clarity (see Supp Fig 1).



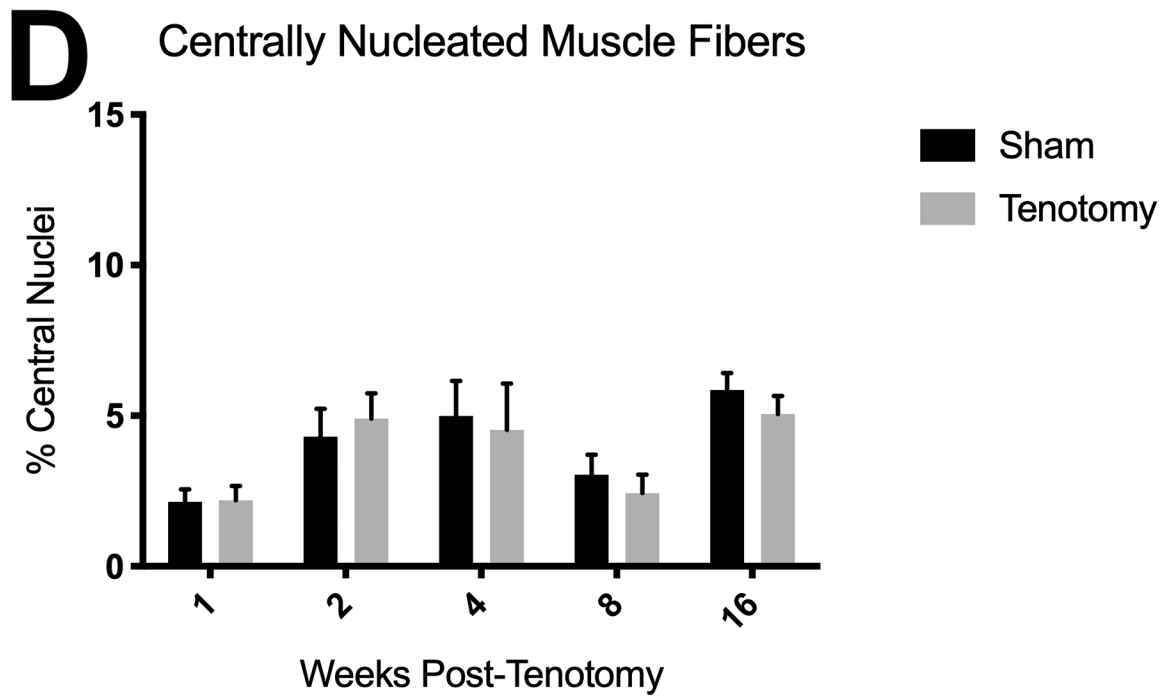
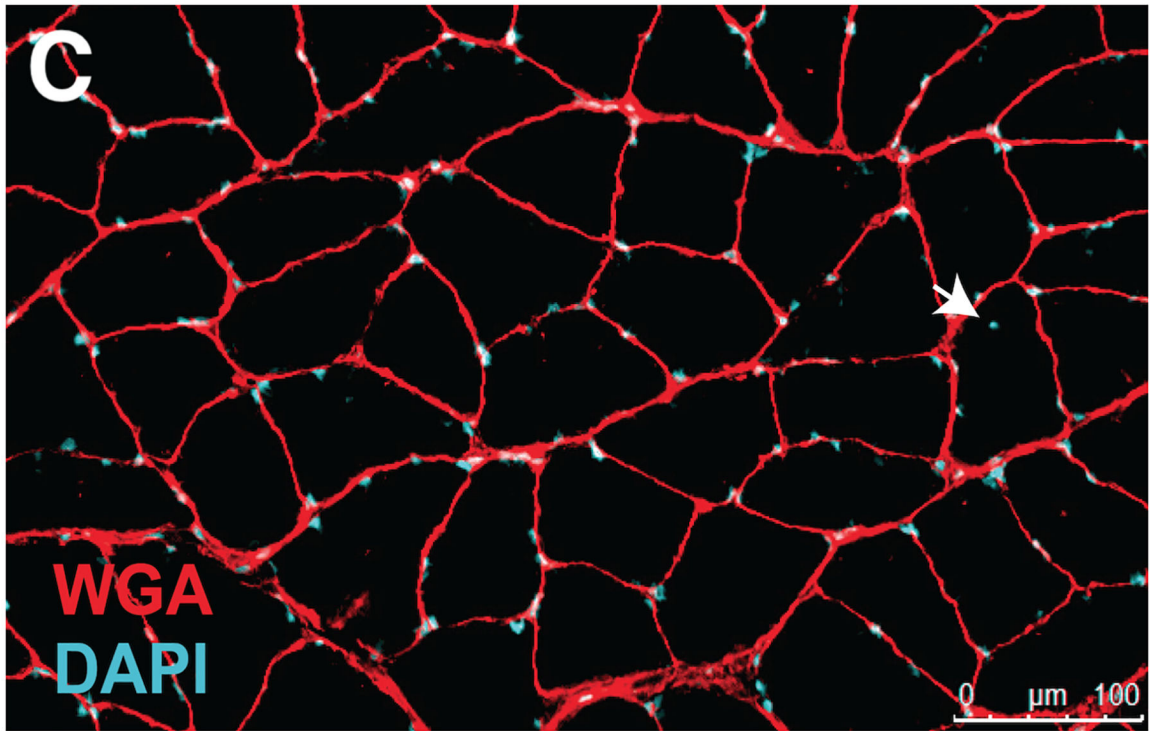


**Fig 4.**

Representative H & E slide at 10X magnification demonstrating signs of muscle fiber degeneration such as hypercellularity (i.e. myophagocytic fibers with multiple non-peripheral nuclei), disrupted muscle fiber membranes, or split muscle fibers<sup>18</sup> (arrows) (Fig 4A). Comparison of muscle degeneration (% of regions showing signs of degeneration)

after tenotomy versus contralateral sham surgery over time (Fig 4B). Wheat germ agglutinin (WGA)-DAPI stain used for quantifying central nucleation (blue dot indicated by white arrow, Fig 4C). Comparison of % muscle fibers with central nuclei in the tenotomy versus contralateral sham surgery groups over time (Fig 4D). Means with standard error shown; horizontal bar denotes  $p < 0.05$  within time point or within treatment group.



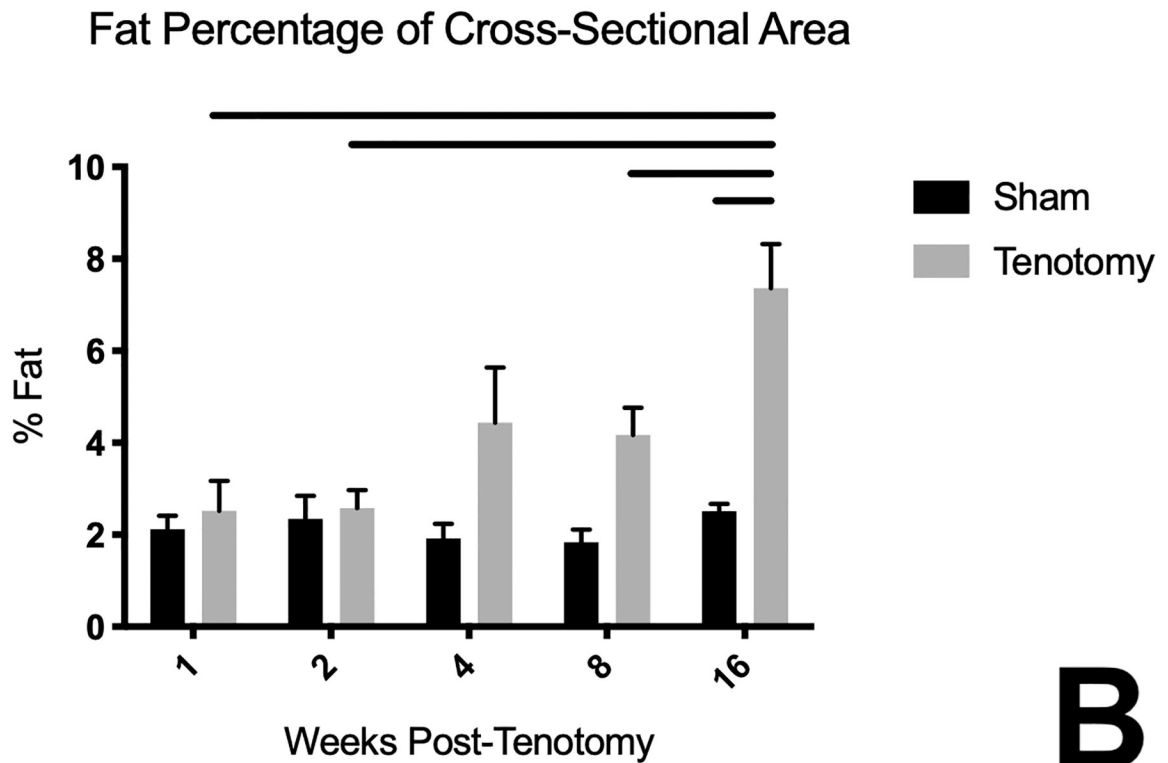
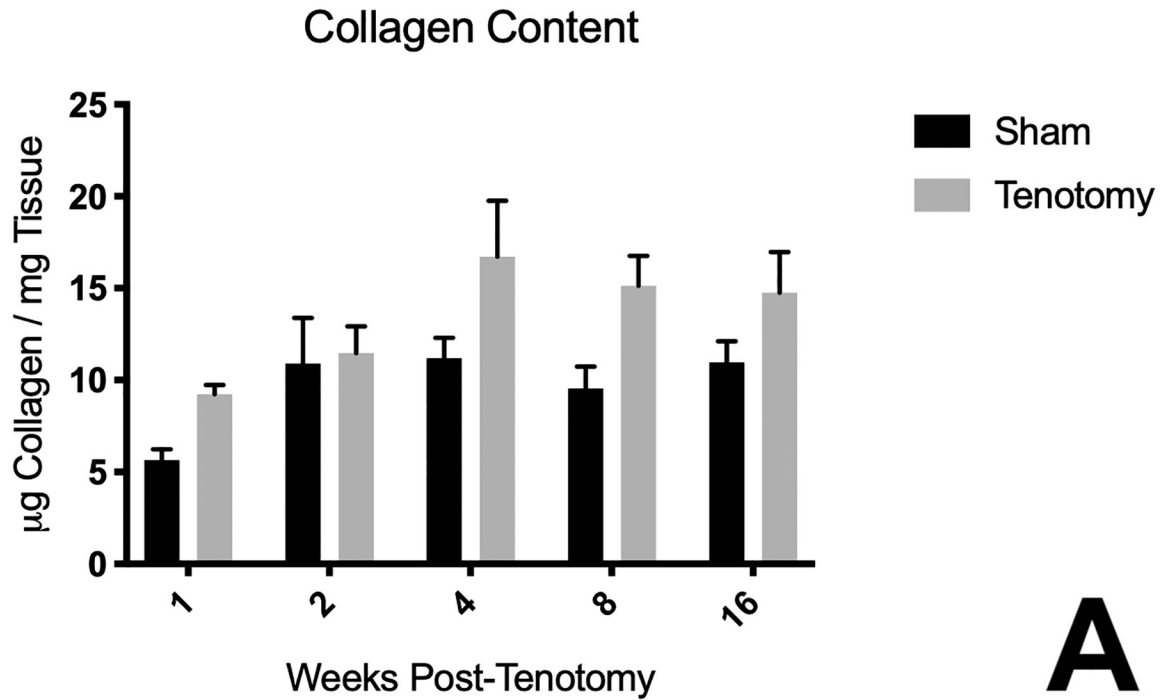


**Fig 5.** Increased collagen (Fig 5A) and fat (Fig 5B) content over time in rabbits post-tenotomy, with significant increase in both components compared to contralateral sham surgery. N=6

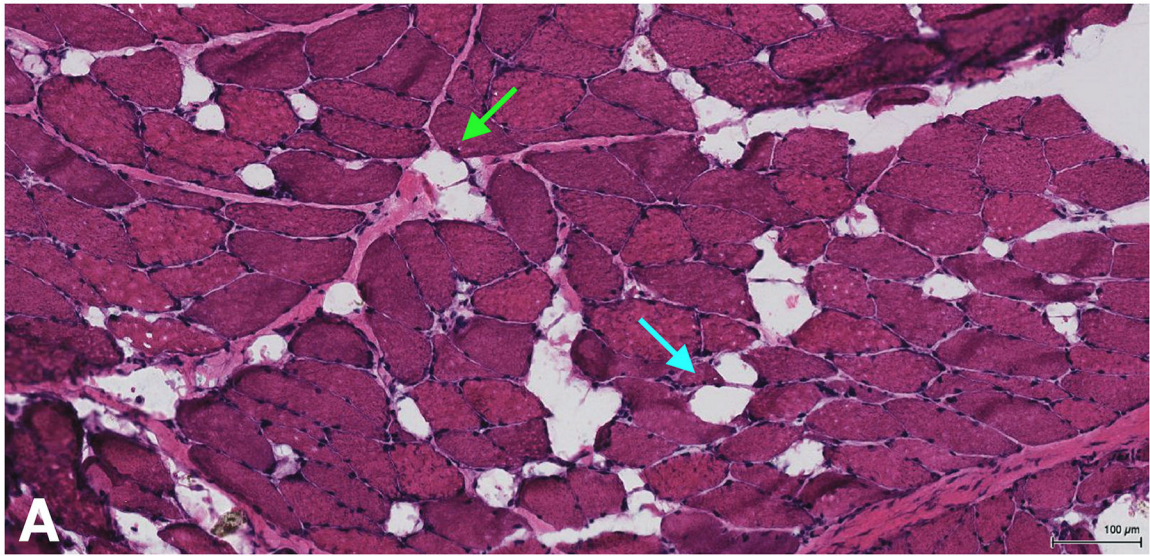
rabbits at each time point. Means with standard error shown; horizontal bar denotes  $p < 0.05$  within time point or within treatment group.

Author Manuscript

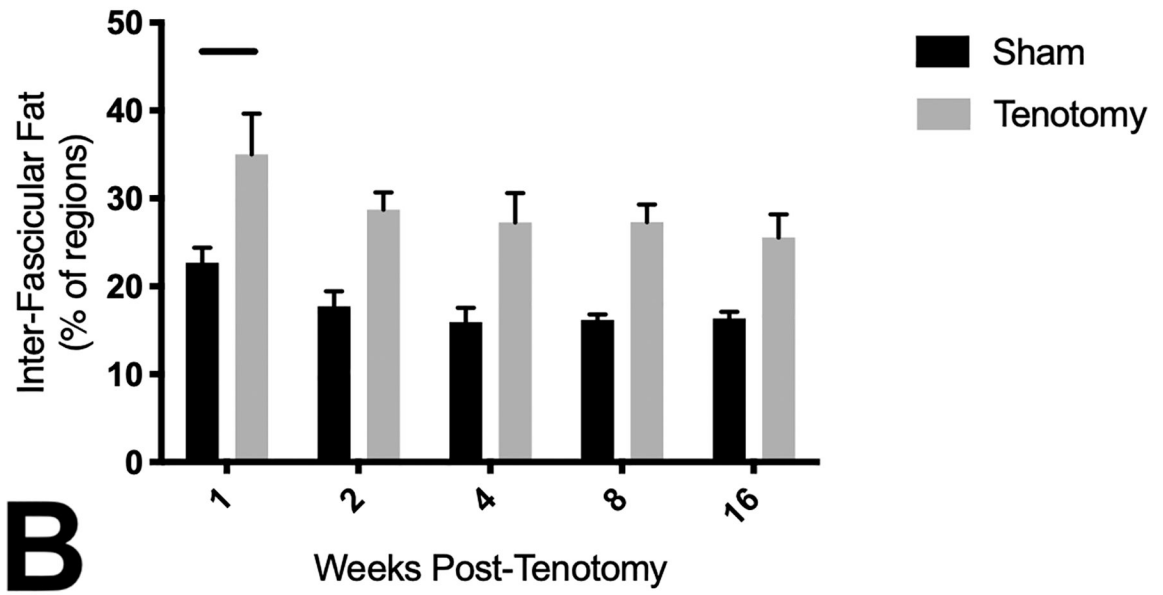
Author Manuscript

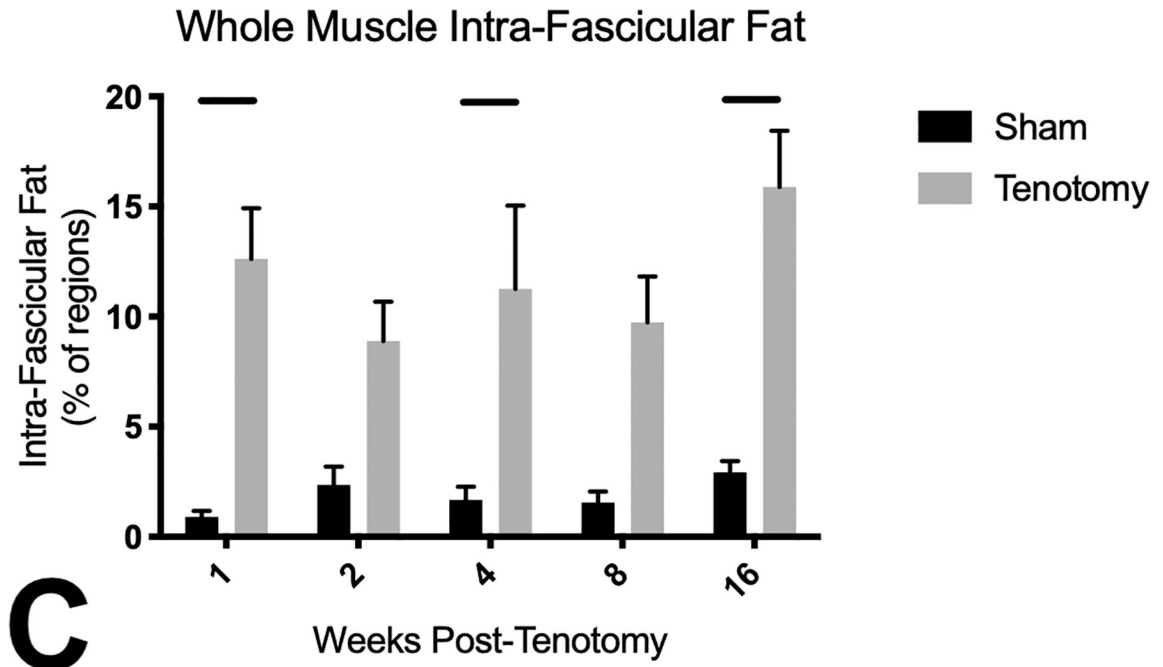
Author Manuscript

Author Manuscript



Whole Muscle Inter-Fascicular Fat



**Fig 6.**

Representative H & E slide at 10X magnification demonstrating inter- (green arrow) and intra-fascicular (blue arrow) fat (Fig 6A). Comparison of inter- (Fig 6B) and intra-fascicular (Fig 6C) fat content at different time points after tenotomy versus contralateral sham surgery. N=6 rabbits at each time point. Means with standard error shown; horizontal bar denotes  $p < 0.05$  within time point or within treatment group.